

# Reports

## Mica Polytypes: Systematic Description and Identification

**Abstract.** *X-ray studies of mica specimens from a variety of geological localities show that biotite and certain lithium-rich mica samples are composed of a mixture of different polytypes. Many of the biotite structures are new complex polytypes not before reported. A new method of designating mica polytypes is proposed. Techniques are described for the systematic generation of all the possible layer-stacking sequences of mica polytypes and for the verification of the stacking sequences in newly discovered forms.*

In order to understand more fully the nature of mica polymorphism, we have systematically examined a large number of mica crystals from a wide variety of geologic localities; established a method of generating all the possible structure models of micas with any given layer repeat, including all pertinent crystallographic data for each model; and developed a method of identifying any particular polytype by analysis of the unit-cell dimensions, space group, structural-presence criteria, and x-ray intensity distribution.

We define the ideal single mica layer as follows: monoclinic; space group,  $C2/m$ ,  $a(3\frac{1}{2}) = b$ ,  $\beta = \cos^{-1}(-a/3c)$ , with the additional special condition that the surface oxygen atoms of the tetrahedral portions of the mica layer are related by a sixfold axis perpendicular to (001). When these symmetry relations obtain, the individual ideal layer can fit exactly upon an adjacent layer in any of six possible orientations, with relative layer rotations about an axis ( $c^*$ ) perpendicular to (001) of  $0^\circ$ ,  $\pm 60^\circ$ ,  $\pm 120^\circ$ , and  $180^\circ$ . Mica polytypism is thus accounted for by arranging  $N$  layers in a particular rotational sequence, the sequence repeating after every  $N$ th layer. Smith and Yoder (1) have presented an elegant graphical method of describing the stacking sequences of the six simplest mica polytypes, namely, the 1M,  $2M_1$ ,  $2M_2$ , 2O, 3T, and 6H forms. The sym-

bols O, T, M, Tc, and H indicate orthorhombic, trigonal, monoclinic, triclinic, and hexagonal symmetry, respectively. We have developed a mathematical method of generating all possible polytypes for a given layer repeat.

In Table 1 are listed the vector stacking symbols, unit-cell parameters, space groups, and structural-presence criteria for all possible 1-, 2-, 3-, and 4-layer mica polytypes. Of the 36 structures represented in this table, all but six (those in large braces) can be identified from a determination of the unit-cell parameters, space group, and structural-

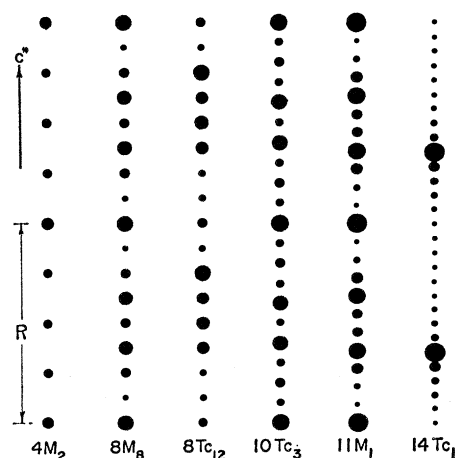


Fig. 1. Representation of the periodic intensity distribution of six new biotite polytypes. The distance  $R$  represents the single-layer repeat of 10 Å.

presence criteria (2). The vector stacking symbols given in Table 1 completely describe the mica structure and represent a new method of designating the mica polytypes. Within the brackets of the stacking symbols are  $N$  numbers, where  $N$  is the number of mica layers per unit cell. The  $j$ th number ( $A_j$ ) of the stacking symbol, where  $j$  designates any particular number in the sequence of  $N$  numbers, refers to the relative angle of rotation between the  $j$ th and  $(j + 1)$ th mica layer. The numbers  $A_j$  can have the values 0,  $\pm 1$ ,  $\pm 2$ , or 3, which refer, respectively, to  $0^\circ$ ,  $\pm 60^\circ$ ,  $\pm 120^\circ$ , and  $180^\circ$  relative rotations of adjacent layers. The vector stacking symbols representing all possible stacking sequences (excluding enantiomorphs) are generated in a systematic way by making all possible non-cyclic, nonredundant (3) permutations of the  $N$  numbers  $A_1 \cdots A_N$  which obey the relation

$$\sum_{j=1}^N A_j = 0 \pmod{6}$$

If  $N > 4$ , the number of possible polytypes is large, thus a computer program has been written to generate the possible models. In Table 2, column A, are listed the number of possible polytypes for layer repeats up to  $N = 6$ .

From our study of the crystallography of more than 200 mica crystals representing a variety of compositions and geologic environments we find that, with one possible exception, micas not bearing lithium possess only ( $0^\circ$ ,  $\pm 120^\circ$ ) stacking sequences (4). Thus, of the possible 1-, 2-, 3-, and 4-layer forms (Table 1), only the 1M,  $2M_1$ , 3T,  $3Tc_1$ ,  $4M_1$ ,  $4M_2$ ,  $4M_3$ , and  $4Tc_3$  polytypes appear to be permissible structures for lithium-free micas. The presence of only the ( $0^\circ$ ,  $\pm 120^\circ$ ) stacking sequences is due to the trigonal symmetry of the surface oxygen atoms of the tetrahedral  $(Si_2O_5)_n^{2n-}$  sheets.

A proper fit of the surface oxygens of adjacent layers is obtained only when the layers are rotated with respect to one another by  $n(120^\circ)$ . Rotations of  $60^\circ$ ,  $180^\circ$ , and  $300^\circ$  do not permit the layers to fit correctly and thus are not found in most mica structures (5). The displacement of the surface oxygen atoms of the  $(Si_2O_5)_n^{2n-}$  sheets from the ideal hexagonal motif to a trigonal one has been noted in all mica crystal structures that have been

accurately refined (5, 6). Apparently, the surface oxygen atoms of lithium-rich micas deviate little from hexagonal symmetry, thus permitting  $\pm 60^\circ$  and  $180^\circ$  as well as  $0^\circ$  and  $\pm 120^\circ$  rotations. Thus far only two mica polytypes have been found that contain  $\pm 60^\circ$  or  $180^\circ$  rotations in the stacking se-

Table 1. Crystallographic data for all possible 1-, 2-, 3-, and 4-layer mica polytypes.

| Vector stacking symbol <sup>a</sup> | $\beta^b$ (deg)   | Space group | Structural-presence criteria   |
|-------------------------------------|-------------------|-------------|--|
| 1M[0]                               | 100.0             | $C2/m$      |  |
| 2O[33]                              | 90                | $Ccmm$      |  |
| 2M <sub>1</sub> [22]                | 95.1              | $C2/c$      | $h3hl:l = 2n+h$  |
| 2M <sub>2</sub> [11]                | 98.7              | $C2/c$      |  |
| 3T[222]                             | 90                | $P3_112$    | $hh2\bar{h}l:l = 3n$   |
| 3M <sub>1</sub> [033]               | 93.4              | $C2/m$      | $0kl:l = 3n$   |
| 3M <sub>2</sub> [112]               | 93.4              | $C2$        |  |
| 3Tc <sub>1</sub> [022]              | 95.1              | $C\bar{1}$  | $\begin{cases} h0l:l = 3n \\ h3hl:l = 3n+h \\ h\bar{3}hl:l = 3n-h \\ 0kl:l = 3n \end{cases}$ |
| 3Tc <sub>2</sub> [011]              | 91.7              | $C1$        |  |
| 3Tc <sub>3</sub> [123]              | 93.4 <sup>d</sup> | $C1$        |  |
| 4O <sub>1</sub> [0303]              | 90                | $Ccmm$      | $0kl:l = 4n$   |
| 4O <sub>2</sub> [1313]              | 90                | $C2cm$      | $h3hl:l = 2n$  |
| 4O <sub>3</sub> [2323]              | 90                | $Ce2m$      |  |
| 4O <sub>4</sub> [1212]              | 90                | $C22_21$    |  |
| 4M <sub>1</sub> [0202]              | 95.1              | $C2/c$      | $\begin{cases} h0l:l = 4n \\ h3hl:l = 4n+2h \\ h\bar{3}hl:l = 4n+2h \end{cases}$             |
| 4M <sub>2</sub> [2220]              | 95.1              | $C2$        | $\begin{cases} h0l:l = 4n \\ h3hl:l = 4n+2h \\ h\bar{3}hl:l = 4n+2h \end{cases}$             |
| 4M <sub>3</sub> [2222]              | 95.1              | $C2/c$      | $\begin{cases} h0l:l = 4n \\ h3hl:l = 4n+2h \end{cases}$                                     |
| 4M <sub>4</sub> [0033]              | 92.5              | $C2/m$      | $0kl:l = 4n$   |
| 4M <sub>5</sub> [1122]              | 92.5              | $C2$        |  |
| 4M <sub>6</sub> [1111]              | 90 <sup>d</sup>   | $C2/c$      | $h3hl:l = 2n$  |
| 4M <sub>7</sub> [0121]              | 90 <sup>d</sup>   | $C2$        |  |
| 4M <sub>8</sub> [0101]              | 98.7              | $C2/c$      | $\begin{cases} h0l:l = 4n \\ 0kl:l = 2n \\ 3hhl:l = 2n+h \end{cases}$                        |
| 4M <sub>9</sub> [1131]              | 94.4              | $C2$        |  |
| 4M <sub>10</sub> [1212]             | 94.4              | $C2/c$      |  |
| 4M <sub>11</sub> [1232]             | 94.4              | $C2$        |  |
| 4Tc <sub>1</sub> [2233]             | 92.5 <sup>e</sup> | $C\bar{1}$  | $0kl:l = 2n$   |
| 4Tc <sub>2</sub> [1122]             | 92.5 <sup>e</sup> | $C1$        | $hhl:l = 2n+h$   |
| 4Tc <sub>3</sub> [1322]             | 92.5 <sup>e</sup> | $C1$        |  |
| 4Tc <sub>4</sub> [0213]             | 92.5 <sup>e</sup> | $C1$        |  |
| 4Tc <sub>5</sub> [0132]             | 92.5 <sup>e</sup> | $C1$        |  |
| 4Tc <sub>6</sub> [1133]             | 90 <sup>d</sup>   | $C\bar{1}$  | $\begin{cases} h0l:l = 2n \\ h3hl, h\bar{3}hl: \\ l = 2n+h \end{cases}$                      |
| 4Tc <sub>7</sub> [0123]             | 90 <sup>d</sup>   | $C1$        |  |
| 4Tc <sub>8</sub> [0022]             | 95.1              | $C\bar{1}$  | $\begin{cases} h0l:l = 4n \\ h3hl, h\bar{3}hl: \\ l = 4n+2h \end{cases}$                     |
| 4Tc <sub>9</sub> [1122]             | 92.5              | $C\bar{1}$  | $hhl:l = 2n+h$   |
| 4Tc <sub>10</sub> [0011]            | 92.5              | $C\bar{1}$  | $hhl:l = 4n+h$   |
| 4Tc <sub>11</sub> [0112]            | 92.5              | $C1$        |  |

<sup>a</sup> The polytypes within the large braces (4M<sub>1</sub>, 4M<sub>2</sub>, 4M<sub>3</sub> and 4Tc<sub>3</sub>, 4Tc<sub>4</sub>, 4Tc<sub>5</sub>) cannot be distinguished from one another with the data given in this table.

<sup>b</sup> The other unit-cell parameters of all of the above polytypes are  $a = 5.3$ ,  $b = 9.2$  Å,  $d_{001} = 10N$  Å (where  $N$  is the layer repeat), and  $\alpha = \gamma = 90^\circ$ —with the following exceptions: 2M<sub>2</sub>, 4M<sub>8</sub>, 4M<sub>9</sub>, 4M<sub>10</sub>, 4M<sub>11</sub> ( $a = 9.2$ ,  $b = 5.3$  Å); 3T (hexagonal  $a = 5.3$  Å,  $\gamma = 120^\circ$ ); 3Tc<sub>1</sub> ( $\alpha = 92.9^\circ$ ); 3Tc<sub>2</sub> ( $\alpha = 98.7^\circ$ ); 4Tc<sub>6</sub>, 4Tc<sub>7</sub> ( $\alpha = 94.4^\circ$ ).

<sup>c</sup> Triclinic polytypes having the special feature of orthogonal (100) projections.

<sup>d</sup> Monoclinic and triclinic polytypes having the special feature of orthogonal (010) projections.

quences, the common 2M<sub>2</sub>[11] lepidolite structure and the 4Tc<sub>5</sub>[0132] lithium fluorophlogopite (7). The number of possible mica polytypes with combinations of  $0^\circ$  and  $\pm 120^\circ$  rotations only are given in Table 2, column B, for layer repeats up to  $N = 9$ .

A study of unusual oxybiotite from a rhyodacite lava flow at Ruiz Peak, New Mexico, has revealed a large number of new mica polytypes. Buerger x-ray-precession photographs of 42 crystals from this material show that approximately one-third are 1M polytypes, one-third 2M<sub>1</sub>, and one-third more complex forms. Among the new complex forms found are 4-, 8-, and 20-layer monoclinic, and 8-, 10-, 14-, and 23-layer triclinic structures. Only a few crystals from this specimen show evidence of random layer-stacking sequences as indicated by apparent continuous or semicontinuous diffuse x-ray scattering parallel to  $c^*$  (8). Our studies of a number of other biotite samples from a variety of igneous and metamorphic rocks suggest that, in general, biotite samples consist of a large number of different polytypes, some so complex as to be unresolved by present x-ray techniques. One biotite sample, however—a specimen from the Tatoosh pluton, Mt. Rainier, Washington (9)—consists, on the basis of an examination of 15 crystals, of only one polytype. A similar study of several lepidolite specimens also indicates the presence of mixtures of polytypes within a single sample. For example, examination of ten lepidolite crystals from Rozena, Czechoslovakia, shows that seven crystals have the 2M<sub>2</sub> structure and three the 1M structure. Identification of particular mica polytypes by the x-ray powder method may thus be invalid unless special precautions are taken to ascertain the homogeneity of the sample.

Among the polytypes listed in Table 1, the 3Tc<sub>1</sub>[022] form was found during our study of a number of siderophyllite crystals from a specimen from a greisen vein, Newcastle County, North Ireland (10). Unit-cell data for this mica are:  $a = 5.35$ ,  $b = 9.27$ ,  $c = 30.17$  Å,  $\alpha = 92^\circ 50'$ ,  $\beta = 94^\circ 58'$ ,  $\gamma = 90^\circ 0'$ , space group  $C\bar{1}$ . The 4M<sub>2</sub>[2220] form was found in the Ruiz Peak oxybiotite specimen and has the following unit-cell parameters:  $a = 5.32$ ,  $b = 9.22$ ,  $c = 40.06$  Å,  $\beta = 95^\circ 5'$ , space group  $C2$ . Takeda and Donnay (7) found the 4Tc<sub>5</sub>[0132] structure during

Series  $(3n+1)[(222)_n 0]$ ,  
 $(3n+2)[(222)_n 2\bar{2}]$

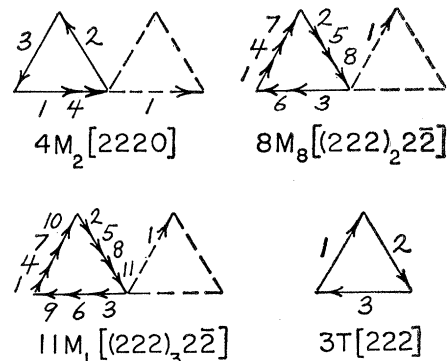


Fig. 2. The stacking sequences of the 3T, 4M<sub>2</sub>, 8M<sub>8</sub>, and 11M<sub>1</sub> polytypes as represented by Smith-Yoder diagrams.

their study of a synthetic lithium fluorophlogopite. The unit-cell data for this polytype are:  $a = 5.31$ ,  $b = 9.19$ ,  $c = 40.0$  Å,  $\alpha = \gamma = 90^\circ 0'$ ,  $\beta = 92^\circ 35'$ , space group  $C1$ . The unit-cell parameters given above compare very favorably with those given in Table 1.

In order to try to solve the structures of the newly discovered mica polytypes we derived the unit-cell parameters, space groups, atomic positions, and structural-presence criteria for all possible 1- to 8-layer models with ( $0^\circ$ ,  $\pm 120^\circ$ ) stacking sequences, as well as for a large number of 10-, 11-, and 14-layer forms. A number of models give the same unit-cell data and presence criteria; thus it is necessary to find a method of analyzing the intensity data obtained from x-ray diffraction patterns. Takeda (11) has developed a special technique of calculating an "unmodulated periodic intensity distribution" that is characteristic of the stacking sequence of each mica polytype. This distribution of intensities is repeated along certain of the reciprocal lattice rows parallel to  $c^*$  after every  $N$  reflections. For mica polytypes with ( $0^\circ$ ,  $\pm 120^\circ$ ) stacking sequences, the  $hkl$  reflections where  $k = (3n+1)$  or  $(3n+2)$  and  $l = m, (m+1) \dots (m+N)$ , where  $m$  and  $n$  are integers, show this characteristic repeat. The periodic intensity distribution is easily distinguished in the x-ray-precession photographs, repeating every  $(10 \text{ Å})^{-1}$  along row lines parallel to  $c^*$ . A comparison of the observed and calculated intensity distribution over  $N$  reciprocal lattice nodes is sufficient to identify the polytype. The periodic intensity distri-

bution of six of the new biotite polytypes is shown in Fig. 1.

The periodic intensity distribution was calculated for approximately 250 models that were generated by the polytype-generation program. We were able to ascertain the stacking sequence of the  $4M_2$ [2220],  $8M_8$ [(222)<sub>2</sub>2 $\bar{2}$ ],  $8Tc_{12}$ [0002 $\bar{2}$ 02], and  $10Tc_3$ [22222 $\bar{2}$ 200] forms from the Ruiz Peak sample and the  $11M_1$ [(222)<sub>3</sub>2 $\bar{2}$ ] form from Lemhi County, Idaho (12). The  $4M_2$ ,  $8M_8$ , and  $11M_1$  polytypes belong to a double series of mica structures which have a crystal structure based on a three-layer trigonal,  $3T$ [222], substructure. These series can be described as having layer repeats of  $N = (3n + 1)$  and  $N = (3n + 2)$  with vector stacking sequences of [(222)<sub>n</sub>0] and [(222)<sub>n</sub>2 $\bar{2}$ ], respectively, where  $n$  is any integer. The stacking sequences, as represented by Smith-Yoder diagrams (1), of the  $4M_2$ ,  $8M_8$ , and  $11M_1$  forms are given in Fig. 2. Another series, represented by the symbol [(0)<sub>n</sub>2 $\bar{2}$ ], appears to be quite common. Polytypes belonging to this series have structures based on the 1M form but with a single 120° periodic stacking fault. Thus far we have

Table 2. Number of possible mica polytypes having any combination of (A) 0°, ±60°, ±120°, and 180° layer rotations, and (B) 0° and ±120° rotations only.  $N$  is the number of layers per unit-cell.

| $N$ | (A) | (B) |
|-----|-----|-----|
| 1   | 1   | 1   |
| 2   | 3   | 1   |
| 3   | 6   | 2   |
| 4   | 26  | 4   |
| 5   | 83  | 8   |
| 6   | 402 | 18  |
| 7   |     | 39  |
| 8   |     | 94  |
| 9   |     | 222 |

Table 3. Characteristic x-ray diffraction spectra of various possible disordered micas.

| Polytype      | Layer rotations                    | X-ray spectra  |
|---------------|------------------------------------|--|
| $1M_r-n(120)$ | Random<br>0°, ±120°                | $hkl: k = 3n$<br>(sharp);<br>$k \neq 3n$<br>(diffuse)                  |
| $1M_r-n(60)$  | Random<br>0°, ±60°,<br>±120°, 180° | $hkl: h$ and $k = 3n$<br>(sharp);<br>$h$ or $k^a \neq 3n$<br>(diffuse) |
| $1M_r-n(180)$ | Random<br>0°, 180°                 | $hkl: h = 3n$<br>(sharp);<br>$h \neq 3n$<br>(diffuse)                  |

<sup>a</sup> Or both.

found the following representatives of this series:  $3Tc_1$ [02 $\bar{2}$ ],  $8Tc_1$ [(0)<sub>2</sub>2 $\bar{2}$ ],  $14Tc_1$ [(0)<sub>12</sub>2 $\bar{2}$ ], and  $23Tc_1$ [(0)<sub>21</sub>2 $\bar{2}$ ].

The origin of diffuse x-ray scattering in x-ray photographs of the micas (8, 13) has been generally attributed to random layer rotations (rotational disorder) within the mica structure. Our experience suggests that "unresolved periodic stacking faults" are a more important origin of the "apparent diffuse scattering." This is particularly evident when sharp subcell spots, sometimes accompanied by weak satellite spots, and apparent diffuse scattering appear in the x-ray photographs. With our present photographic techniques we cannot resolve a repeat of much more than 300 Å. With a special collimation system we hope to increase this to 600 Å. Also, natural mica crystals generally show mechanical distortion, thus making it difficult to obtain ideal diffraction patterns. An example of the periodic intensity distribution of a mica that is believed to have a single periodic stacking fault is shown by the  $14Tc_1$  structure of Fig. 1.

One biotite specimen (Brooks Mountain, Alaska) (14) shows very even semicontinuous diffuse scattering parallel to  $c^*$  for those  $hkl$  reciprocal lattice rows for which  $k \neq 3n$ . No sharp subcell spots appear. We believe that this mica structure has rotational disorder in the classical sense (13), the streaking being caused by random  $n(120^\circ)$  layer rotations. We designate mica polytypes with such structures as  $1M_r-n(120)$  where 1M refers to the 1M substructure,  $r = \text{random}$ , and  $n(120)$  refers to random 0°, 120°, and 240° rotations. Theoretically, other types of rotational disorder may occur, namely, random  $n(60^\circ)$  and  $n(180^\circ)$  rotations. We will designate such possible disordered mica polytypes as  $1M_r-n(60)$ , and  $1M_r-n(180)$ , respectively. The nature of the x-ray scattering expected from these three possible polytypes is given in Table 3. The  $1M_r-n(120)$  form is quite common in biotites and perhaps in fine-grained authigenic micas. The  $1M_r-n(180)$  structure is not expected to occur and is of only theoretical interest.

With our present experience concerning the occurrence of the various mica polytypes, plus that of others (1, 8), we suggest the following distribution of mica polytypes in relation to chemical composition: biotites—mixtures of many polytypes with (0°, ±120°) stack-

ing sequences including the  $1M_r-n(120)$  form; muscovites and paragonites— $2M_1$ , very rarely  $3T$ ; lithium micas—1M,  $2M_1$ ,  $2M_2$ ,  $3T$ , plus mixtures of these simple forms, rarely more complex polytypes; authigenic micas—1M, less commonly  $2M_1$ , possible  $1M_r-n(120)$ ,  $1M_r-n(60)$ , and two-dimensional (15) forms. The relation between polytypism, chemical composition, and geologic occurrence, of paramount importance, requires further study.

MALCOLM ROSS

HIROSHI TAKEDA†

DAVID R. WONES

U.S. Geological Survey,  
Washington, D.C. 20242

#### References and Notes

- J. V. Smith and H. S. Yoder, *Mineral Mag.* 31, 209 (1956).
- Reflections from trioctahedral micas that violate the structural-presence criteria in general have an intensity so weak as to be unobservable by conventional film methods. Dioctahedral micas usually produce some observable x-ray reflections that violate the presence criteria. They are, however, as a class always very weak. Thus, it is easy to differentiate them from the generally strong reflections which do obey the presence criteria.
- For example, cyclic permutations of a stacking sequence such as [0123] give the identical sequences [1230], [2301], and [3012]. The negative and reverse permutations of the sequence [0123] give the identical sequences (neglecting enantiomorphs) [0 $\bar{1}$ 2 $\bar{3}$ ], [3210], and [ $\bar{3}$ 2 $\bar{1}$ 0]. Also, a sequence of numbers such as [2222] does not represent a possible four-layer polytype, for there is a 2 $\bar{2}$  subrepeat. Rather, it represents a two-layer form with the stacking sequence [22].
- All these crystals show the structural presence criterion  $h0l: l = 0 \text{ mod } N$  which is characteristic of mica structures that do not possess any ±60° or 180° layer rotations. Also, due to the pseudotrigonal symmetry of these mica structures the  $h3l$  and  $h\bar{3}l$  photographs are nearly identical with the  $h0l$  photographs and thus show the same presence criterion.
- E. W. Radoslovich, *Acta Cryst.* 13, 919 (1960).
- H. Steinfink, *Am. Mineralogist* 47, 886 (1962); Y. Takéuchi and R. Sadanaga, *Acta Cryst.* 12, 945 (1959); C. W. Burnham, *Carnegie Institution of Washington Yearbook* 63, 232 (1964); G. Donnay, N. Morimoto, H. Takeda, J. D. H. Donnay, *Acta Cryst.* 17, 1369 (1964).
- H. Takeda and J. D. H. Donnay, *Program and Abstracts*, Amer. Cryst. Assoc. winter meeting, 24–26 February 1965, Suffern, N.Y., p. 23.
- S. B. Hendricks, *Phys. Rev.* 57, 448 (1940); *Am. Mineralogist* 24, 729 (1939).
- T. L. Wright, *ibid.* 49, 715 (1964).
- S. R. Nockolds and J. E. Richey, *Am. J. Sci.* 237, 27 (1939).
- Manuscript in preparation.
- D. E. Lee, *Am. Mineralogist* 43, 107 (1958).
- A. J. C. Wilson, *X-ray Optics* (Methuen, London, 1949), pp 45–63.
- R. R. Coats and J. J. Fahey, *Am. Mineralogist* 29, 373 (1944).
- By the two-dimensional form we mean crystals so thin in the  $c$ -direction that the intensity distribution consists only of continuous diffuse scattering along all reciprocal lattice rows parallel to  $c^*$  ( $hk$  rods). No basal (001) reflections will appear in the x-ray photographs.
- We thank Prof. J. D. H. Donnay for interest and advice. One of us (H.T.) carried out a part of this study at the Crystallographic Laboratory, Johns Hopkins University, under NSF grant GP 1565. Publication authorized by the director, U.S. Geological Survey.
- Present address: Mineralogical Institute, University of Tokyo, Tokyo, Japan.